Trends of Thermal Structure in the MLT Region Using SABER Observations Over Sutherland, South Africa

Blessing Mvana Nhlozi[1], Sifiso Ntshangase[1], Nkanyiso Mbatha[2], Makhosonke Dubazane[3]

[1]Department of Physics, University of Zululand, KwaDlangezwa 3886, South Africa
[2]Holistic Climate Change, CSIR, Pretoria 0001, South Africa
[3]Discipline of Physics, University of KwaZulu-Natal, Westville 3630, South Africa

E-mail: `mvanablessing@gmail.com`

Abstract. The Mesosphere and Lower Thermosphere (MLT) region, located between the stratosphere and ionosphere, plays a critical role in atmospheric dynamics and space weather coupling. Using long-term temperature data from the Sounding of the Atmosphere using Broadband Emission Radiometry (SABER) instrument, this study investigates trends in the thermal structure of the MLT over Sutherland, South Africa. The aim is to characterize regional variability in response to solar and anthropogenic influences. Results reveal altitude-dependent cooling trends, with statistically significant long-term cooling observed in the 56–80 km and 100–107 km ranges, while the 90–100 km layer remains dynamically unstable with no clear trend. Seasonal cycles are prominent, with cold-point shifts and temperature anomalies linked to transient dynamical processes. A Physics-Informed LSTM model successfully captures seasonal variability and underlying trends, offering a physically consistent forecast of near-future temperature evolution.

1 Introduction

The Mesosphere and Lower Thermosphere (MLT) region, situated between the stratosphere and the ionosphere, is a crucial atmospheric layer that plays a vital role in energy exchange, atmospheric dynamics, and space weather interactions. One of the key observational tools for studying the MLT region is the Sounding of the Atmosphere using Broadband Emission Radiometry (SABER) instrument, which provides long-term temperature measurements to investigate trends and variations in atmospheric parameters [1].

Research shows that the MLT region is experiencing long-term temperature changes due to solar cycle effects, greenhouse gas cooling, and atmospheric wave propagation [2]. However, more localized studies are needed to better characterize regional differences in MLT region temperature trends, particularly in the Southern Hemisphere [3].Despite advancements in lidar and satellite-based diagnostics, simultaneous storm-time observations of temperature and winds in the MLT region remain sparse. This limitation highlights the need for localized studies, such as those conducted over Sutherland, South Africa, to bridge gaps in understanding neutral dynamics during geomagnetic disturbances[**?**]. Sutherland, South Africa, is a strategic location for studying MLT region temperature trends due to its unique atmospheric and geographic characteristics.

To investigate these dynamics, this study uses SABER data to assess MLT region temperature trends over Sutherland. It applies both classical statistical techniques (e.g., Mann–Kendall, Sen's slope) and modern deep learning (DL) approaches, including Physics-Informed Neural Networks (PINNs). The goal is to identify altitude-dependent trends, quantify long-term variability, and test the feasibility of DL models. Ultimately, this work aims to address two key challenges: closing the data gap in Southern Hemisphere MLT studies and exploring whether advanced DL techniques can meaningfully enhance trend detection and forecasting in the upper atmosphere.

2 Methodology

The SABER instrument onboard National Aeronautics and Space Administration's Thermosphere, Ionosphere, Mesosphere, Energetics and Dynamics (TIMED) satellite has been routinely measuring temperature since 2002. We used the level-2 temperature data, which was downloaded from SABER's website. The data was then manipulated by first filtering it with a bounding box that was centered over Sutherland, which is located at 32.4°S, 20.8°E. The data was run through a data pipeline, which cleaned and created several databases based on the type of aggregations. After it goes through the pipeline, it then undergoes statistical and ML processes.

2.1 Statistical Trend Detection

The MK test is used to determine the presence of monotonic trends, and the Sequential Mann–Kendall (S-MK) test to identify the onset point of such trends. These non-parametric methods are ideal for climate data where distributional assumptions may not hold. A backward sequence was computed.

2.2 Deep Learning

DL was used to capture nonlinear interactions and enhance physical interpretability; we implement a PINN framework based on Yao et al. [4]. The network used SABER temperature data, using LSTM. Training is typically performed using Adam optimizers. To ensure physical consistency, we incorporate PINN constraints during training. For example, the time series showed Second-order linear ordinary differential equations (ODEs) behavior thus a nonhomogeneous ODE was imposed directly into the network through an additional physics-based loss term, using sen slope as trend in the nonhomogeneous ODE.

3 Results and Discussion

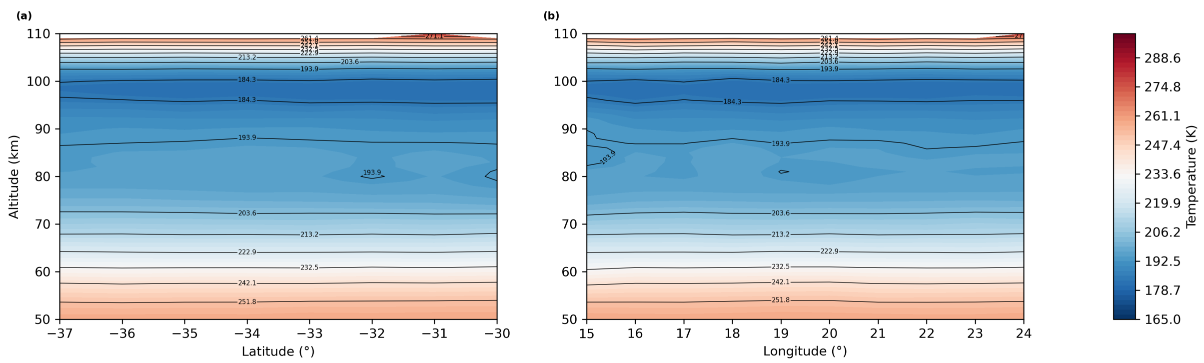

Figure 1: *Altitude versus Coordinates showing SABER temperature observations. (a) Zonal cross-section showing temperature variation with altitude and latitude. (b) Meridional cross-section showing temperature variation with altitude and longitude. Contour lines overlaid on color-filled contours highlight temperature gradients in the mesosphere and lower thermosphere. Data from SABER observations. The colorbar shows temperature in Kelvin.*

The MLT region is well stratified, as seen in Figure 1, with the cold layer (mesopause) between 95 and 100 km denoted by a noticeable thermal inversion. As is typical of a well-defined inversion layer, this layer, which is the coldest region of the atmosphere, is bounded by rising temperatures both below (mesosphere) and above (lower thermosphere). The absence of prominent horizontal anomalies suggests on average their is a minimal planetary wave influence over the past 22 years, indicating relatively stable atmospheric conditions. However, temporal analysis in Figure 2 suggest otherwise, revealing multiple periods of abrupt thermal shifts indicative of transient dynamical influences.

Gravity wave breaking, which promotes upward momentum deposition and long-wave radiative cooling, is probably what keeps the cooling at the mesopause going. The temperature increase above 102 km can be the result of increased Joule dissipation or tidal heating, especially during times of intense geomagnetic activity. The stratified thermal structure observed over Sutherland is consistent with solstice-driven mesospheric circulation and may be enhanced by the site's high elevation (1.8 km), which favors gravity wave propagation into the MLT.

Figure 2 provides a time–altitude visualization with no consistent long-term trend indicative of climate change is apparent in the temperature field. While downward shifts of the cold point occur in isolated months, these are

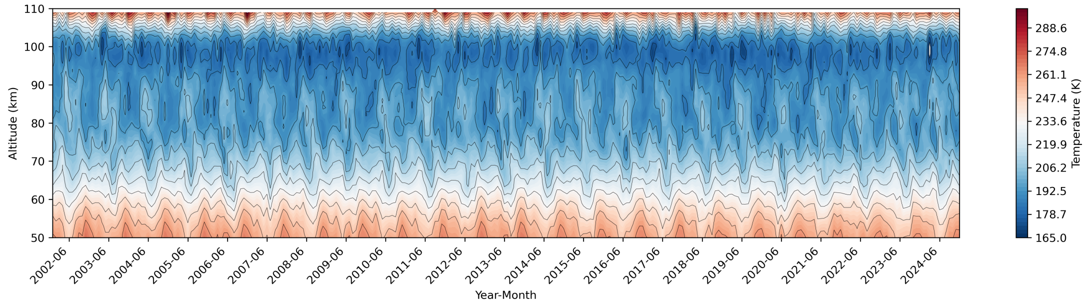

Figure 2: *Time–Altitude cross-section of monthly mean temperature (2002–2025). Color-filled contours show temperature in Kelvin (K), with overlaid black contour lines for structure. X-axis represents time (June months from 2002 to 2024), and Y-axis shows altitude levels (50–109 km). This plot reveals temporal and vertical variability in the MLT region.*

episodic rather than part of a persistent trend. A well defined seasonal cycle is evident, with the cold point intensifying and shifting to lower altitudes during the winter (June–July) and warming in summer (December–January) reflect strong seasonal modulation. Increased upwelling and adiabatic cooling, which are traits of winter mesospheric dynamics in the Southern Hemisphere, are consistent with this behavior.

The cold point exhibits significant vertical and temporal change between 75 and 103 km, changing in depth, altitude, and intensity, underscoring the mesopause's dynamic character. In contrast, temperature structures near the lower and upper bounds of the profile are more thermally stable. However, several episodes break this seasonal regularity. For example, notable anomalies in 2007, 2013, and 2016, when the cold point weakens is followed by abrupt cooling in early 2018, may be linked to external drivers such as the Quasi-Biennial Oscillation (QBO), solar variability, or sudden stratospheric warmings.

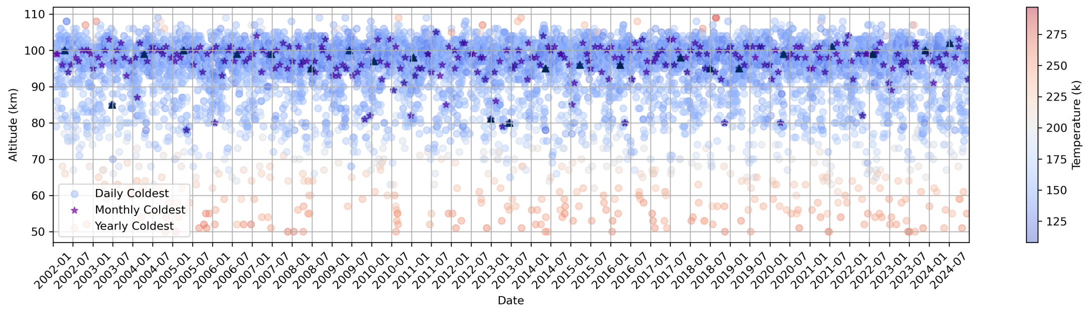

Figure 3: *Temporal distribution of coldest temperature points between 2002 and 2024. Daily cold points (circles), monthly averages (stars), and yearly minima (triangles). The vertical position represents the altitude bin where the minimum temperature was found, and the color intensity corresponds to the coldest temperature recorded in each temporal group.*

A clear clustering is shown in Figure 3, which Monthly minima (stars) are concentrated in the 95–105 km range, while the majority of cold points are located between 90 and 105 km. Periodic monthly cold spots below 90 km are probably caused by dynamic anomalies or temporary mesospheric inversions. In December 2004, July 2005, May–June 2009, June 2010, and a few months in 2012–2019, there are rapid decreases to 80 kilometers. These occurrences could be mesospheric disruptions or localized cold air invasions. The importance of seasonal extremes is further supported by the fact that yearly cold points (triangles) are more common during the warmer months of December through February. Anomalies below 85 km, including those in December 2012 and January 2003, point to anomalous cooling or exceptional mesopause descent. The absence of yearly minima during most of 2007 and 2013 may reflect data gaps, quality filtering, or unusually stable mesospheric conditions during those years.

The Sequential Mann-Kendall (SMK) test uses statistical curves called UF (forward sequence) and UB (reverse sequence) to find patterns and potential change points in a time series. The junction of the UF and UB curves and whether or not they cross a crucial threshold, often ±1.96, define the existence, direction, and time of statistically significant trends. It shows no significant overall trend in mean monthly temperatures in the MLT (UF end = +0.096). The final UF and UB values are well within the non-significant range, indicating that no consistent, significant trend is present in the entire temperature time series in the MLT region. However, the large number of cross points suggests localized or intermittent trends. Multiple trend shifts suggest that rather than a long-term growth or fall, the data may show quasi-periodic or oscillatory behavior. Nevertheless, discrete areas of statistically significant cooling are shown by elevation-resolved analysis. Consistently low UF values and a large number of cross sites support a strong and statistically significant cooling trend in the 76–85 km range, suggesting a structural shift in the temperature field. The layer between 100 and 107 km also shows a noticeable but weaker cooling trend. However, there is no discernible trend in the 90–100 km region, which is consistent with the observed irregularity in cold point positioning and further points to dynamic instability in this layer.

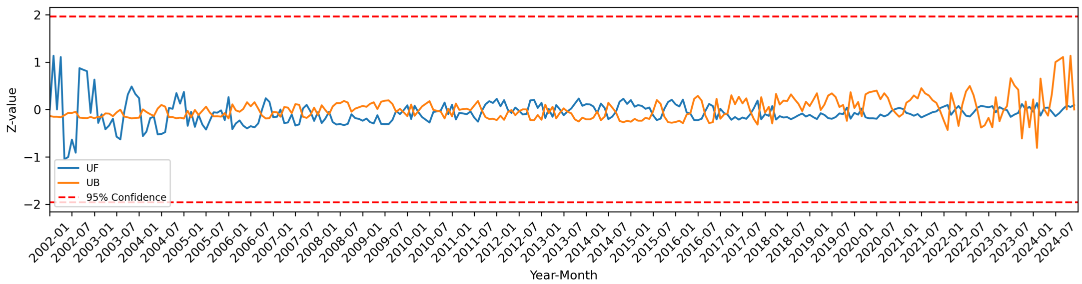

Figure 4: *Sequential Mann-Kendall (SMK) trend test between 2002 and 2024. The UF (forward sequence) and UB (backward sequence) statistics are plotted over time. The red dashed lines mark the 95% confidence interval bounds (±1.96). Intersections between UF and UB within the confidence bounds may indicate trend reversals, while sustained crossings above or below indicate statistically significant monotonic trends. X-axis labels are shown at 6-month intervals for clarity.*

Table 1: *Altitude-Resolved Temperature Trends from the Sequential Mann-Kendall (SMK) Test. The table summarizes trends across five altitude bands, based on the terminal UF values and their statistical significance.*

Altitude Range (km)	Trend	UF End Value	Significance
50-55	None	-1.42 to -1.87	Not significant
56-75	Cooling	-1.97 to -3.18	Strong
76-80	Cooling	-1.90 to -2.70	Moderate
81-99	None	-0.60 to -1.70	Not significant
100-109	Cooling	-1.60 to -1.88	Mild to Moderate

For lags 1–5, residual ACF is: [0.329 0.170 -0.029 0.094 -0.018]

With warm peaks regularly appearing in December or January and chilly minima in June or July, the graph in Figure 5 clearly illustrates an annual seasonal cycle that closely resembles the seasonal behavior depicted in Figures 1–3. Longer-term temperature undulations seem to be influenced by a secondary solar-related fluctuation in addition to this fundamental seasonal modulation. While Figure 4 did not show any monotic trend.

A weak long-term cooling trend is apparent over the two-decade period, though it is partially obscured by short-term fluctuations and inter annual variability. For instance, a warming event from July to November 2017 is abruptly followed by a sharp temperature drop in January 2018, suggesting transient forcings such as planetary wave intrusions or mesospheric disturbances. The MLT's susceptibility to transient dynamics is further highlighted by repeated irregular fluctuations from February to May, which may indicate increased short-term variability or transitional atmospheric states. Extreme temperatures typically cluster in the summer and winter months (January and July, respectively), which is consistent with other data.

To quantify the background tendency, a linear trend line was derived using Sen's slope estimator from the MK trend test. This trend is also used as a physics-informed constraint within the loss function of a Physics-Informed LSTM (PI-LSTM) model, aiming to stabilize training on nonhomogeneous ordinary differential equations. The red line in Figure 4 shows the PI-LSTM forecast extending from January 2025 to December 2026. The model takes into account the learned trend and seasonal structure and extrapolates it forward, offering a physically consistent forecast rather than a purely data-driven one.

The PI-LSTM model shows strong short-term predictive skill (as seen from RMSE, MAE, and Forecast Skill Score), especially compared to a naïve baseline. The NSE is negative, indicating that some outliers or quick changes are not effectively recorded, even while the skill score (about 0.48), which shows moderate prediction gain over a persistence model, is positive.

Despite its poor raw accuracy metrics, the model's strong seasonal monitoring and forecasting structure make it a great tool for qualitative insights and anomaly detection across multi-month periods. NSE and MASE, however, indicate that it may not adequately capture the seasonal structure or long-term trend because of the intrinsic variability in MLT dynamics and its limited feature set.

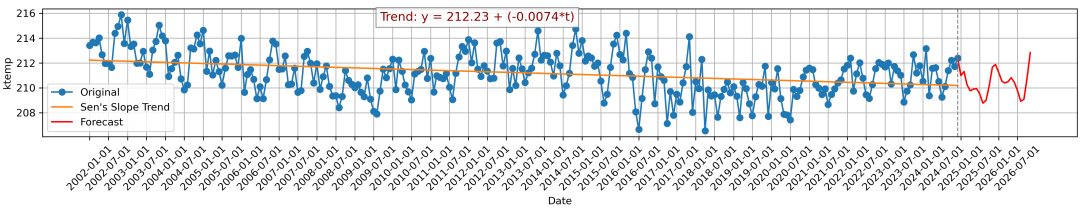

Figure 5: *Time series of observed temperature, overlaid with Sen's slope trend estimate and a 24-month forecast generated using a Physics-Informed Long Short-Term Memory (PI-LSTM) model. The vertical dashed line marks the transition from observed data to forecasted values. The linear trend equation, derived from Sen's slope, is displayed on the plot. This visualization highlights past temperature variability, estimated monotonic trend, and the model's prediction of near-future temperature evolution.*

Table 2: *Model performance metrics comparing the PI-LSTM model to a naïve baseline (last value persistence).*

Metric	**Value**	**Interpretation**
Mean Absolute Error	0.1176	Average monthly error is 0.12 units, indicating low deviation.
Mean Squared Error	0.0203	This low MSE supports the MAE result.
Root Mean Squared Error	0.1423	Similar to MAE but more sensitive to large errors.
Mean Absolute Percentage Error	29.44%	Model errors are 29% of actual values, typical for noisy data.
Symmetric MAPE	31.50%	Moderate performance, common for noisy geophysical data.
Mean Absolute Scaled Error	1.1192	Ideally, MASE should be <1.
Nash-Sutcliffe Efficiency	-0.1540	The model performs worse than the mean prediction.
Skill Score (vs. baseline)	0.4846	Model is 48.5% better than the naïve forecast.
Forecast Skill Score (FSS vs. naïve)	0.9797	Excellent skill compared to naïve forecast. Nearly perfect.
Quantile Loss (q=0.9)	0.3150	Model is reasonably good at predicting upper-bound temperatures
Pinball Loss (q=0.9)	0.09069	Measures accuracy of quantile forecast; lower is better.
Dynamic Time Warping (DTW)	0.5052	Thier is high similarity between predicted and actual sequences.

4 Conclusion

4.1 Summary

Using SABER satellite observations from 2002 to 2024, the present investigation examined seasonal patterns and long-term temperature trends in the MLT region above South Africa. Five altitude bands between 50 and 109 km were examined for statistically significant trends in mesospheric temperature using the SMK test. With peak magnitudes falling between 56 and 75 km, the results show a steady and noteworthy cooling trend in the 56–80 km range. While lower altitude (50–55 km and 81–99 km) do not display any statistically significant long-term trends, upper altitudes (100–109 km) show lesser but noticeable cooling.

Seasonal and interannual variations were prominent, especially during the months of July and January, which typically coincide with extrema in temperature anomalies. A notable anomaly occurred between July and November 2017, where temperatures surged sharply before dropping again in early 2018.

Using a Physics-Informed Long Short-Term Memory (PI-LSTM) model, the forecasting potential of deep learning techniques was investigated. Strong predictive performance was shown by the model, which was able to accurately capture seasonal cycles and the declining temperature trend over time. The stability and interpretability of the model were further enhanced by adding physical restrictions to the loss function.

4.2 Future Work

Several directions are proposed for future research. First, incorporating additional physical drivers such as solar flux indices, QBO, and geomagnetic activity may improve the model's ability to distinguish natural variability from climate trends. The Trend-Run model developed by Bencherif et al. [5] is considered to simulate MLT temperature trends as a function of major climate drivers. Thus, the Multiple Linear Regression (MLR) Model. Second, extending the spatial domain beyond South Africa to include other midlatitude and tropical sites could help generalize the model and reveal regional differences in mesospheric climate response. Taking into account supplementary studies such piecewise regression for multiple trend phases, wavelet transform for non-stationary cycles, and Empirical Mode Decomposition (EMD) in the event that nonlinear trends are suspected.

From a modeling standpoint, the depiction of temporal dependencies may be enhanced by additional PI-LSTM design optimization using methods like attention mechanisms or encoder-decoder schemes. Last but not least, merging observational data with ground-based or reanalysis datasets may enhance vertical resolution and lower observational uncertainty, opening the door for integrated frameworks for climate forecasting in the upper atmosphere.

References

[1] T.-Y. Huang and M. Vanyo, "Trends in the Airglow Temperatures in the MLT Region—Part 2: SABER Observations and Comparisons to Model Simulations," *Atmosphere*, vol. 12, p. 167, 2021.

[2] T. T. Ojo, Z. T. Katamzi-Joseph, K. T. Chu, M. A. Grawe, and J. J. Makela, "A climatology of the nighttime thermospheric winds over Sutherland, South Africa," *Advances in Space Research*, vol. 69, no. 1, pp. 209–219, 2022.

[3] X. R. Zhao, Z. Sheng, H. Q. Shi, L. B. Weng, and Q. X. Liao, "Long-term trends and solar responses of the mesopause temperatures observed by SABER during the 2002–2019 period," *Journal of Geophysical Research: Atmospheres*, vol. 125, no. 11, 2020.

[4] Y. Yao, X. Zhong, Y. Zheng, and Z. Wang, "A physics-incorporated deep learning framework for parameterization of atmospheric radiative transfer," *Journal of Advances in Modeling Earth Systems*, vol. 15, no. 5, p. e2022MS003445, 2023.

[5] H. Bencherif, V. Sivakumar, and R. Jimmy, "TREND-RUN model for performing the trend calculation on SAWS (South Africa Weather Service) atmospheric data," in *28th Annual Conference of South African Society of Atmospheric Sciences*, Sep. 2012, pp. 90–91.